铜/钛合金电子束焊接工艺优化

刘 伟, 陈国庆, 张秉刚, 冯吉才
(哈尔滨工业大学 现代焊接生产技术国家重点实验室, 哈尔滨 150001)

摘 要: 研究了 QCr0.8/TC4 电子束焊接工艺及接头组织, 由于铜合金热导率高而熔化量较小, 以及焊缝中生成大量脆性金属间化合物相, 因此对中焊时接头强度较低。采用偏铜侧进行非对中电子束焊接, 接头抗拉强度随偏束量的增大而增高, 偏束量为 0.8 mm 时接头最高抗拉强度为 270.5 MPa。断裂发生在 TC4 侧熔合线处, 为脆性准解理断裂特征。偏铜焊时接头成形得到改善, 焊缝包括熔合区及 TC4 侧反应层两部分。熔合区主要由铜基固溶体组成, 硬度较 TC4 母材有所降低。反应层成分过渡较大, 含有多种金属间化合物相。随着工艺参数的变化, 反应层厚度也发生变化, 从而对接头性能产生影响。

关键词: QCr0.8 合金; TC4 合金; 电子束焊; 工艺优化
中图分类号: TG456.3 文献标识码: A 文章编号: 0253-360X(2008)05-0089-04

刘 伟

0 序 言

随着航空航天、机械工程和仪器制造等领域科研工作的深入开展, 要求越来越多不同性能的结构和部件结合应用, 这就涉及到大量异种材料连接工艺方面的问题[1]。铜及其合金具有优良的导电导热性、延展性和抗腐蚀性能, 某些铜合金还具有较高的强度, 因而在工业生产中得到广泛的应用[2]。钛合金是一种传统的结构材料, 其综合性能良好, 尤其符合航空航天、船舶和汽车制造行业结构减重的要求[3]。然而铜与钛的互溶性很小, 物理和化学性能存在较大差异, 在焊接热作用下极易形成 Ti_xCu_y 型脆性金属间化合物, 还易形成低熔点共晶物, 焊接性较差。铜和钛都属于活泼金属, 在常温和高温时极易氧化, 高温时吸收氢和氮的能力较大, 焊缝中易形成氢气孔和氢化物 TiH_2, 从而引起氢脆。有关铜与钛及其合金的连接当前的一些研究结果集中在固相焊接领域, 例如采用钎焊、扩散焊、摩擦焊、爆炸焊及热轧焊等方法[4-8]。Meshram 等人[6] 研究了铜/钛摩擦焊接, 结果表明焊缝成形良好, 接头最高抗拉强度可达 228 MPa。Kahraman 等人[7] 研究了铜/钛板材爆炸焊接头组织和力学性能, 发现炸药量较大时连接处形成了细晶组织。扫描电镜显示连接处没有金属间化合物的生成, 拉伸和剪切均断裂在铜母材侧。然而, 针对常见的平板对接接头, 固相连接存在叠加增重、接头形式特殊和使用温度低等不足, 应用受到一定限制。

文中研究了 QCr0.8 铬青铜与 TC4 钛合金电子束焊接接头组织及力学性能, 重点采用偏束焊接改善接头组织, 提高力学性能。

1 试验方法

试验所用材料分别为 QCr0.8 铬青铜和 TC4 钛合金(Ti-6Al-4V), 两种母材的化学成分及力学性能如表 1 所示。

表 1 母材的化学成分(质量分数, %)和力学性能

Table 1 Chemical constitutions of base metal (wt. %) and their mechanical properties

母材	Cr	Al	V	Ti	Cu	其它	抗拉强度 R_m/MPa	断后伸长率 A(%)
QCr0.8	0.4~0.7	—	—	—	余量	≤0.8	360	≥25
TC4	—	6.2	3.5	余量	—	≤0.2	931	10

收稿日期: 2008-01-10

母材的金相组织如图 1 所示。QCr0.8 合金为 α+

(α+Cr)亚共晶组织,其中基体为 α—Cu 相,灰色颗粒状为Cr 相,如图 1a 所示。图 1b 为 TC4 合金组织形貌,由典型的 α—Ti 相和 α+β 网状组织组成。

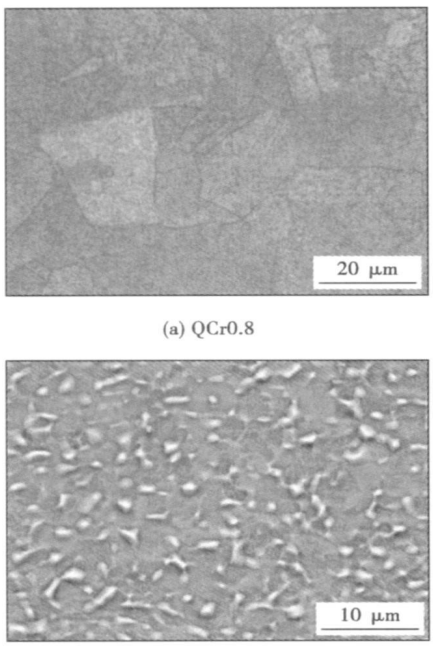

图 1 母材的微观组织形貌

Fig. 1 Microstructure of base metal

待焊试件的尺寸为 50 mm×30 mm×2 mm,焊前采用机械方法清理试件,用丙酮或无水乙醇清洗表面。焊接设备为 MEDARD —45 型脉冲真空电子束焊机,应用自制夹具将待焊试件夹紧固定,在真空度为 5×10^{-2} Pa 时进行焊接。

焊后接头组织结构观察在 PME OLYMPUS 型光学显微镜下进行;接头的抗拉强度在 INSTRON MODEL1186 电子万能试验机上进行;采用 X 射线衍射仪(XRD, D/max—rb 旋转阳极)分析焊缝的相组成;采用扫描电镜(SEM, S—4700)分析焊缝组织及断口的形貌特征;通过能谱仪(EDS, TN—4700)测定各反应相成分;用数字式显微硬度计(HXD —1000TM)对接头区域进行硬度分析。

2 结果分析

2.1 QCr0.8/TC4 对中焊

QCr0.8/TC4 电子束对中焊接头强度较低,这与焊缝组织结构及反应产物密切相关。由于铜合金的导热性能明显优于钛合金,因而铜母材熔化量较少。QCr0.8 和 TC4 两种不同材料熔合成的焊缝不同于其中某一个母材组织,其典型的焊缝微观组织形貌如图 2 所示。由图可见熔池从液态首先结晶出粗大的树枝晶,几乎横贯焊缝。后析出相在其间长大,遇阻后形成细小针状相。析出相将杂质和低熔点共晶物排向晶界,此外还有一些颗粒相分布在晶界处。

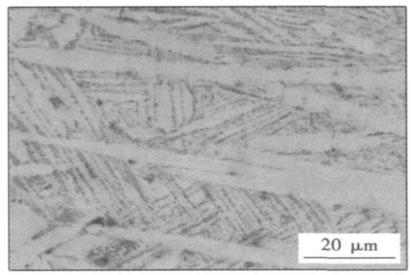

图 2 对中焊焊缝组织形貌

Fig. 2 Weld structure by centered EBW

由 Ti—Cu 二元相图可知,两种元素极易形成金属间化合物,从而降低了焊缝的塑韧性。分别对不同焊接热输入的试件进行了拉伸测试,结果如图 3 所示。由图可见,对中焊时接头抗拉强度在 90 ~ 120 MPa 之间,仅为 QCr0.8 母材的 30%左右,接头强度相对较低。

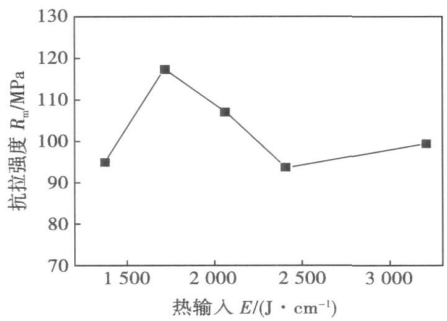

图 3 焊接热输入与接头抗拉强度的关系

Fig. 3 Relationship between heat input and tensile strength

2.2 非对中焊接头力学性能

由于铜母材参与焊缝组成量较少,将电子束下束位置向铜侧偏移以增大铜熔化量。试验设定加速电压为 55 kV,束流为 35 mA,焊接速度为 8 mm/s,仅改变偏束量来研究其对非对中焊接头质量的影响,结果如图 4 所示。可以看出相对于对中焊,非对中焊接头抗拉强度大幅提高,在偏束量为 0.8 mm 时,接头获得了最高的抗拉强度 270.5 MPa。接头强度产

生这种具有峰值变化特征主要是由焊缝化学成分、组织结构及铜/钛界面反应程度决定的，主要体现在熔合区共晶或化合物的生成量及界面反应层的厚度上。

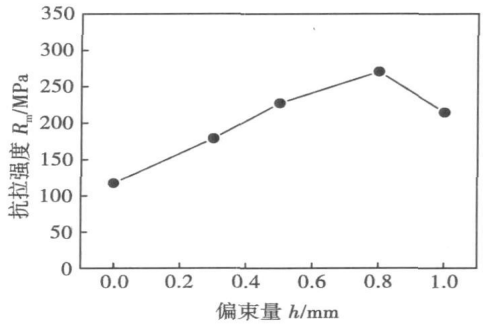

图 4　偏束量对抗拉强度的影响

Fig. 4　Influence of lateral deviation quantity on tensile strength

对偏束量为 0.8 mm 接头的硬度分布进行了分析，沿接头横截面的水平方向，测试了焊缝、热影响区及母材区域，测试结果如图 5 所示。接头两侧热影响区(HAZ)的硬度分布与两侧母材基体相近，说明热影响区处的组织并未显著粗化。由于是偏铜侧进行焊接，焊缝中含有较多的铜基固溶体，因而硬度较低，仅稍高于铜合金母材。而在 TC4 侧反应层处硬度过渡剧烈，在应力作用下易在熔合区或反应层处发生断裂。

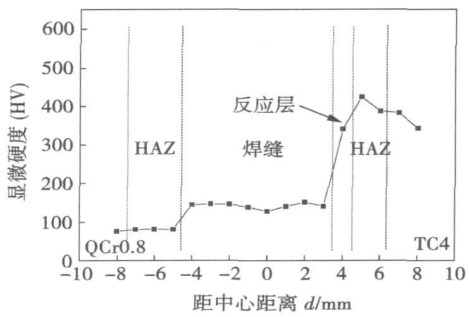

图 5　非对中焊接头硬度分布特征

Fig. 5　Hardness distribution of joints by non-centered EBW

非对中焊接头断裂特征如图 6 所示。图 6a 为接头的断裂位置，断裂发生在靠近钛合金侧的反应层中。由于铜基固溶体含量增加，组织的塑韧性略有提高，断裂性质为脆性准解理断裂，且在断口附近存在二次裂纹，如图 6b 所示。

2.3　非对中焊接头组织分析

由力学性能分析结果可知，在电子束的偏束作用下接头组织结构发生了显著变化，焊缝由原来的

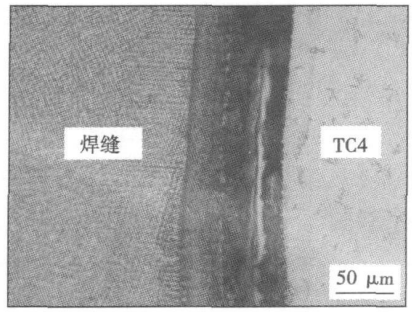

(a) 断裂位置

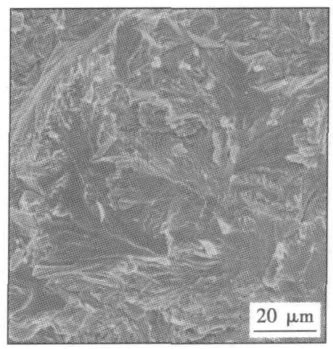

(b) 断口形貌

图 6　非对中焊接头断裂位置和断裂特征

Fig. 6　Fracture location and characteristic of joints by non-centered EBW

硬脆化合物组织转变为以铜基固溶体为基体的组织，从而使接头力学性能得到改善。

从化学成分及组织构成上分析认为，偏 QCr0.8 进行电子束焊接时，由于存在较多的铜基固溶体相，使焊缝的塑韧性明显得到改善。当偏铜量较小，焊缝中由于 Ti 元素含量增加而生成较多的低熔共晶和化合物，在凝固过程中被排挤到晶界处，在焊接热应力作用下容易形成结晶裂纹，如图 7 所示。随着偏铜量的增加，Ti 元素熔化和溶解变少，晶间共晶和化合物也相应的减少，使得焊缝的塑韧性明显提高，强度增加。当偏铜量过大时，铜/钛界面处易出

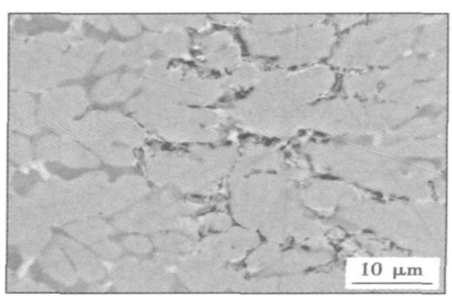

图 7　焊缝结晶裂纹形貌

Fig. 7　Crystal crack in weld

现气孔缺陷,且由于能量的减少,界面处冶金结合变差。

断口 X 射线衍射分析结果如图 8 所示,结果表明断口或反应层中含有铜基固溶体,CuTi 及 $CuTi_3$ 等。由于反应层含有较多的 Ti 元素而使该处生成较多的金属间化合物 CuTi 及 $CuTi_3$,化合物在生成过程中由于成分偏析将 Cu 元素排向熔池,凝固结晶成一薄层。分析认为,偏铜电子束焊试件断裂均发生在反应层中的富铜层处,由于铜基固溶体的存在一定程度上缓解了反应层的脆性,因此,虽然断裂仍发生在反应层,但强度有了明显的提高。

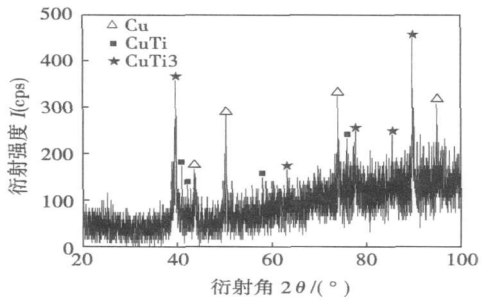

图 8 断口 X 射线衍射分析结果

Fig. 8 Fracture analysis by XRD

从界面反应方面分析,当偏铜量较小时,由于铜/钛界面处有较多的原子扩散和溶解,界面反应层较厚,并产生较大的应力集中而使接头变脆。随着偏铜量的增加,界面处的原子扩散与固溶程度有所降低,使得反应层厚度减小,应力集中较小而有利于强度的提高。当偏铜量为 0.8 mm 时,反应程度及反应层厚度适中,因此强度达到最大值。偏铜量过大时由于能量消耗,使得界面反应不充分而难以实现良好的冶金结合,因此强度较低。

3 结 论

(1) QCr0.8/TC4 电子束对中焊接头组织为粗大的树枝晶,晶间分布着杂质和低熔点共晶物,接头抗拉强度普遍较低。

(2) 非对中焊接头抗拉强度大幅提高,在偏束量为 0.8 mm 时最高抗拉强度达到 270.5 MPa。焊缝硬度相对较低,断裂发生在 TC4 侧反应层附近,为脆性准解理断裂。

(3) 非对中焊焊缝组织以铜基固溶体为主,断口或反应层中含有铜基固溶体,CuTi 及 $CuTi_3$ 等,反应层的厚度随工艺参数而改变,从而影响到接头的力学性能。

参考文献:

[1] 李亚江, 王 娟, 刘 鹏. 异种难焊材料的焊接及应用[M]. 北京: 化学工业出版社, 2003.

[2] 黄伯云, 李成功, 石力开, 等. 中国材料工程大典, 第 4 卷[M]. 北京: 化学工业出版社, 2006.

[3] Oh J, Kim N J, Lee S, *et al*. Correlation of fatigue properties and microstructure in investment cast Ti—6Al—4V welds[J]. Materials Science and Engineering, 2003, A340: 232—242.

[4] Shiue R K, Wu S K, Chan C H. The interfacial reactions of infrared brazing Cu and Ti with two silver-based braze alloys[J]. Journal of Alloys and Compounds, 2004, 372: 148—157.

[5] 赵熹华, 韩立军, 杨 泉. 钛合金和铜合金扩散焊接接合区形貌研究[J]. 焊接学报, 1997, 18(12): 12—16.

[6] Meshram S D, Mohandas T, Reddy G M. Friction welding of dissimilar pure metals[J]. Journal of Materials Processing Technology, 2007, 184: 330—337.

[7] Kahraman N, Gülenc B. Microstructural and mechanical properties of Cu—Ti plates bonded through explosive welding process[J]. Journal of Materials Processing Technology, 2005, 169: 67—71.

[8] Ruge J. Joining of copper to titanium by friction welding[J]. Welding Journal, 1986, 65(8): 28—31.

作者简介: 刘 伟, 男, 1970 年出生, 博士研究生, 副教授。主要从事新材料、异种材料电子束焊接及数值模拟方面的研究工作。发表论文 10 余篇。

Email: liuwei @hit.edu.cn

results with material coupling of Q235—Q235 indicate that the temperature distribution on the friction surface has a tendency to rise gradually from the inside to outside on radial direction during welding process, while the contact pressure distribution decreases gradually. With the increase of rotary speed, the temperature is remarkably increased while the material doesn't illustrate obvious plastic deformation, but the effect is relatively weak with the increase of temperature. When material in the contact zone illustrates plastic strain at high temperatures, increasing axial force is more effective for increasing temperature and inducing large deformation.

Key words: friction hydro pillar processing; friction stitch welding; finite element method; thermal-mechanically coupled analysis

Mechanical properties and welding parameters window of friction stir welding WANG Wei, SHI Qingyu, LI Ting, LI Hongke (Advanced Materials Processing Technology, Ministry of Education, Tsinghua University, Beijing 100084, China). p77—80

Abstract: Friction stir welding parameters play an important role of figuration and mechanical properties of welded joint. In this study, the 3 mm plate of 2024 aluminum alloy was selected as base metal. By operating a great deal of butt welding experiments, the quality of welded joint under various parameters was tested. Furthermore, the welding parameters window was established. In the parameter of rotation speed 375—475 r/min and welding speed 150—235 mm/min, the tensile strength of welded joint can be higher than 80% of the one of base metal. By analyzing the tensile fracture, at the upper district of joint, the material had good plastic aspect, while the lower district was worse than the upper one. The joint showed distinct layers along the depth.

Key words: friction stir welding; aluminum alloy; mechanical property; welding parameters window; fracture

Technological effect on bead characteristics of homemade thick plate welded by high power laser with filler wire TANG Zhuo, ZHAO Lianglei, CAI Yan, WU Yixiong (School of Materials Science & Engineering, Shanghai Jiaotong University, Shanghai, 200240, China). p81—84, 88

Abstract: The high power density of laser makes laser welding process become one of the most promising and efficient welding method. The high power laser welding with filler wire of 10 mm and 12 mm thick plates was studied, and the plasma behavior was analyzed as well. The results showed when the laser power is over 13 kW, the penetration curve becomes gentler and the gradient declines obviously. However, in regard to the fully-penetrated seam, it could not fully demonstrate the effects of the welding parameters on the cross-section only with width and penetrations of the weld bead. The cross-section of fully-penetrated bead appears to be a Y shape. And this kind of Y shape is further designed to be a combination with an inverted trapezoid on the top and a rectangle below. In this way, wire feeding rate and gap are varied in order to study their effects on the Y shape bead dimensions while laser power and welding speed keeping constant. In addition, the influence of plasma of the protective gas was studied.

Key words: homemade thick plate; high power laser; laser welding with fillet wire; weld appearance

Effect of leads pitch on soldered joint reliability of QFP device with finite element analysis SHENG Zhong, XUE Songbai, ZHANG Liang, GAO Lili (College of Materials Science and Technology, Nanjing University of Aeronautics and Astronautics, Nanjing 210016, China). p85—88

Abstract: Finite element method was used to simulate the residual stress in soldered joints of QFP device with the same distance and number of leads, respectively. The results indicated that the stress concentration areas in soldered joint locate at the heel and toe of the soldered joint, as well as at the area between the lead and the soldered joint; the largest value of the stress was in the heel of the soldered joints, which would be the weakest area of the joints. Through the comparison of these results, especially the analysis of stress curves, it was shown that stress increased periodically due to the accumulation of residual stress. In the QFP device with the same number of lead, the stress was increasing in the order: TQFP64< VQFP64< SQFP64. In the QFP devices with the same distance of leads, the increasing of stress was in the order: QFP64< QFP44< QFP32. Comparing with QFP100 at the same time, it was shown that the soldered joint reliability of high density fine pitch device is more qualified.

Key words: finite element method; residual stress; distance of lead; number of lead

Investigation on process optimization of Cu/Ti electron beam welding LIU Wei, CHEN Guoqing, ZHANG Binggang, FENG Jicai (State Key Laboratory of Advanced Welding Production Technology, Harbin Institute of Technology, Harbin 150001, China). p89—92

Abstract: QCr0.8/TC4 electron beam welding process and the structure of joints were studied. The melting quantity of Cu alloy was lower due to its high thermal conductivity; moreover, there were lots of brittle intermetallic compounds in the weld, so the tensile strength of the joint was low. The non-centered electron beam welding was used to improve the tensile strength of Cu/Ti joints. It was indicated that the tensile strength was increasing as the lateral deviation quantity increasing, and the maximum value, 270.5 MPa was obtained when the lateral deviation quantity was 0.8 mm. The fracture occurred near TC4 side, and it was quasi-cleavage crack. The weld was consisted of fusion zone and reaction layer near TC4 side. The fusion zone was mainly consisted of Cu-based solid solution with lower hardness than TC4. In the reaction layer, the component transition was obvious, and there were lots of intermetallic compounds. The thickness of the reaction layer was changed as the process parameter being varied, which influenced the mechanical properties of the joint.

Key words: QCr0.8 alloy; TC4 alloy; electron beam welding; process optimization

Microstructures and properties in simulated heat-affected zone of copper-bearing age-hardening steel LIU Wenyan[1,2], WANG Lai[1], LIU Jibin[2], ZHANG Yunyan[2], LI Pinghe[2], YUAN